Test and Calibration of 20 FBG based strain transducers

F. Klug, H. Woschitz
Graz University of Technology

Abstract

For Structural Health Monitoring applications, several types of strain transducers and measuring systems are commercially available. But choosing the most appropriate system for an individual application is a difficult task as the specifications provided by different manufacturers are often incoherent, incomplete and thus hardly comparable. Independent experiences are useful and thus widely appreciated.
In order to find the most appropriate sensor type for a specific application we have tested four different types of commercially available FBG based strain transducers, produced by three different manufacturers. Several 100 to some thousands sensors of these types are used around the world. Using our calibration facility for fiber optic strain sensors, we applied known strains of up to 10 000 µm/m to the sensors and measured their response. We found large non-linearities of up to 2 500 µm/m in the low strain regions and hysteresis effects of up to 36 µm/m at higher strains. Sensors with a pre-tensioned fiber have shown the largest errors. Subsequently, we calibrated a set of 15 strain transducers of the same type. Although for each of these sensors an individual calibration protocol was delivered by the manufacturer, errors of up to 100 µm/m were found.
This paper shows the test and calibration results of 20 strain transducers and provides independent information about their performance and the size of measuring errors. The results clearly show the need for standards in precise fiber optic sensing where at least some basic quality parameters should be defined.

1. Introduction

For structural health monitoring (SHM) and geotechnical applications a wide range of sensor systems is available. Among them are fiber optic (FO) measurement systems which for example provide high accuracy, need relatively low installation efforts, have low power consumption and show good long term stability. One state of the art technology are fiber Bragg grating (FBG) based systems with many types of commercially available sensors, e.g. for measuring strain, temperature or load. Different manufacturers provide sensors and/or reading units. In most cases the available sensor specifications are not consistent, or are fragmentary, why choosing the most appropriate sensor for a specific application is difficult.
Within this paper we show calibration results of a variety of FO strain transducers of different manufacturers. The measurements were carried out with a unique calibration facility which was developed and built at our institute (Engineering Geodesy and Measurement Systems, IGMS). Wavelengths we measured using a dynamic interrogator based on swept wavelength technology with a resolution of 1pm. Using the calibration results, we show systematic effects of the different FBG strain transducers which degrade accuracy. By this we highlight the practical problems that arise due to a lack of dedicated standards.

2. Fiber Bragg Gratings

In this section we briefly repeat some base knowledge about FBG technology, as some sensor manufacturers refer to literature for the conversion from raw data to strain and do not provide any additional information.
FBG sensors are formed by periodic changes of the refractive index in the core of an optical fiber which reflects part of the light transmitted in the fiber. The center wavelength of the reflected signal λ_B can be determined from the Bragg condition (e.g., Othonos & Kalli, 1999)

$$\lambda_B = 2 \cdot n_{eff} \cdot \Lambda \qquad (1)$$

with the effective refractive index n_{eff} and the period Λ of the refractive index changes. It is affected by strain (ε) and temperature (T) changes and the wavelength shift induced by these quantities is often (e.g. VDI/VDE 2660-1) approximated by the linear function

$$\frac{\Delta\lambda_{(\varepsilon,T)}}{\lambda_B} = k_\varepsilon \cdot \varepsilon + k_T \cdot \Delta T \qquad (2)$$

with the normalised strain (k_ε) and temperature (k_T) sensitivity. Typical values are $k_\varepsilon = 0.78$ and $k_T = 6.67 \cdot 10^{-6}$/K (Peters, 2009). As a temperature change of 1 K and a strain change of 8 µm/m almost yield the same measurement signal at wavelengths of approximately 1550 nm, temperature correction of the strain values is crucial for precise measurements. This is often realised by an FBG temperature sensor that is placed in the vicinity of the strain sensor.
When it comes to wavelength to strain conversion, some manufacturers refer to "typical values" but do not give a specific reference. Thus we now want to focus on the variety of k_ε and k_T values in the literature. In recent literature k_ε varies from 0.77 (Udd & Spillman, 2011) to 0.80 (Berghmans & Geenaert, 2011) and k_T from $6.67 \cdot 10^{-6}$/K (Peters, 2009) to $8.86 \cdot 10^{-6}$/K (Spillman & Udd, 2014). Kashyap & López-Higuera (2002) collected older values ($0.61 \leq k_\varepsilon \leq 0.79$, $6.3 \cdot 10^{-6}\text{/K} \leq k_T \leq 8.2 \cdot 10^{-6}$/K). As the exact composition of the fiber material is often missing, both in literature and in specifications of commercial strain transducers, the practical user can be confused, which one of the values to use. But as the variation of the coefficients is about 25% and a wrong coefficient may result in errors of several 100 µm/m, this is an important issue, when discussing accuracy. Compared to this, errors caused by modern interrogators which offer strain resolutions at the 1 µm/m level seem to be negligible.
Furthermore, it often is not clear to the practical user, if these values can be used for ready to use sensors too, where the basic sensing element is used together with other materials, e.g. parts for connecting the fiber to the anchor or parts for fiber protection and thus other effects might be superimposed.
Another practical issue is the mechanical strength which is limited by the breaking limit of the glass fiber and the FBG sensor respectively. Many manufacturers specify a strain limit of about ±5 000 µm/m. Draw tower gratings (DTG), which are produced on a draw-tower prior to the coating process, provide higher limits which almost correspond to the one of a standard fiber (Rothhardt et al., 2004) and seem to be more appropriate for sensing than their classical counterparts.

3. IGMS calibration device for fiber optic strain transducers

For the investigation of FO strain transducers, we have developed a unique facility within the last years (Presl, 2009). Fig.1a shows a schematic diagram of this facility, Fig.1b its realization.
Key components are a linear translation stage, which allows a maximum sensor elongation of 300 mm, and a laser interferometer that is used as a reference measurement system. Different types of FO strain sensors can be tested or calibrated, like ready to use strain transducers, strain sensor cables used for distributed sensing or even bare fiber sensors used for special applications. Basically, the facility was intended for long gauge strain sensors with minimum lengths of about 15 cm which will be embedded or surface mounted. For the investigation of very small sensors, which are directly attached to a structure using different kinds of epoxy, other specialised facilities exist (Habel et al., 2011), and may be used if needed. The unique performance parameters of our facility are its length, which allows using sensors of up to 30 m length without folding.

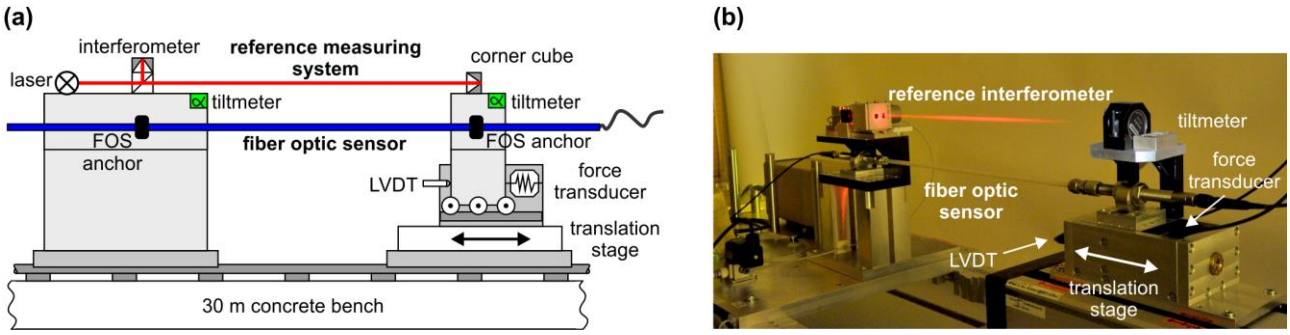

Figure 1: (a) schema and (b) realization of the testing and calibration facility for FO strain transducers in the IGMS metrology laboratory

For bare fiber sensors, a pneumatically driven fiber clamp is used (Presl, 2009), for other sensors like strain transducers specific clamping adapters can be used with the facility. As some strain transducers (e.g. SOFO type, Inaudi et al., 1994) have a relatively long set-up, the interferometer and the FOS had to be set-up eccentrically by about 65 mm and by this Abbe's comparator principle could not be fulfilled. Thus, to avoid errors due to this fact, two tiltmeters are used for monitoring the alignment stability of the two anchor platforms. For fatigue testing, a force transducer (max. 2 kN) can be used which is mounted inside a special housing on the translation stage. Little movements caused by the sensing membrane of the force transducer do not affect the interferometer measurements due to construction principles. After sensor set-up and definition of the strain testing profile, the facility provides fully automatic operation and data acquisition. It is set up in a temperature and humidity controlled laboratory of our institute on a rail system mounted at a stable, 30 m long, concrete bench. This bench is separated from the laboratory's floor and the base of the building in order to reduce vibration effects induced by these elements. Of course, a longer FOS is supported at several points in order to avoid significant sagging. Temperature is monitored by five PT100 sensors along the concrete bench and usually remains stable within 0.1 K during the calibration period. The accuracy of the facility depends on the sensor length and the maximum strain applied to it. For example, for a 5 m long strain transducer which is strained for 30 000 µm/m, the expanded standard uncertainty of the reference system (determined in accordance to GUM, JCGM, 2008) is about $U_{\Delta L} = \pm 2.5$ µm ($k = 2$) for the measured length changes ΔL. This corresponds to an expanded standard uncertainty in strain of about $U_\varepsilon = \pm 0.5$ µm/m.

4. Investigated FBG-strain transducers

In this paper we show the results of 20 different FBG strain transducers produced by three different manufacturers. Most of them (15) are of the same type and were later used within a monitoring project of a hydro power dam (Klug et al., 2014). The other sensors were used only in our laboratory within these investigations.
Figure 2 shows a schema of the investigated strain transducers, which is in principle the same for all investigated transducer types. All of them are intended for both, embedment and surface mounting.

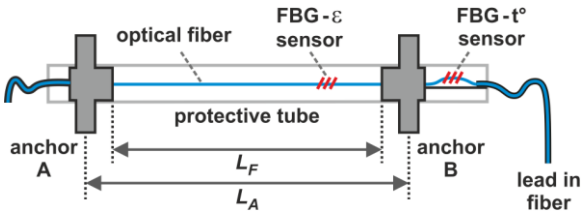

Figure 2: Schema of the investigated strain transducers

The fiber with the strain sensing FBG is attached to two anchors and protected by a flexible tubing. It is either pre-tensioned in order to allow negative strains too, or in the case of a loose fiber inside the tubing, the strain transducer needs to be pre-tensioned during installation.
The length of the strain transducer usually is specified as the length L_A between the two anchors, however, the free fiber length (L_F) might be different. This is an important fact for sensor calibration and for applications where measured strain is converted to length changes ΔL.
The basic specifications and the number of tested sensors are listed in Table 1. The sensors from manufacturer A (two different types) were ordered with a rather low pre-strain (about 200 µm/m), those from manufacturer B were produced without pre-strain and those from manufacturer C have a fixed pre-strain of 5 000 µm/m. Some of the strain transducers (manuf. A and C) can be ordered with an additional temperature sensitive FBG for the temperature correction of the measured strain values, others (manuf. B) do not have this option.

Table 1: Overview of investigated strain transducers

manufacturer	sensor type	length L_A	temperature compensating FBG	number of tested sensors
A	I	0.5 m	built-in	15
	II	0.5 m	built-in	1
B	III	0.5 m	-	1
		1.0 m	-	1
		2.0 m	-	1
C	IV	0.5 m	built-in	1

The available information was collected for all sensor types and the specifications regarding accuracy are listed in Table 2. Without further information, a comparison like this might be used for choosing the proper sensor.

Table 2: Specifications of the investigated strain transducers (source: data sheets of the manufacturers)

manufact-urer	sensor type	sensing element	operating range [µm/m]	pre-tension [µm/m]	accuracy [µm/m]	precision [µm/m]	repeatability [µm/m]	hysteresis [µm/m]	non-linearity [µm/m]	strain conversion
A	I	DTG	±5 000	selectable	1.8	1	N/A	N/A	N/A	individual calibration
	II	DTG	±5 000	selectable	N/A	1.7	N/A	N/A	N/A	individual calibration
B	III	DTG	-5 000 to 10 000	0 or 5 000	N/A	1	N/A	N/A	N/A	N/A ($k_\varepsilon = 0.78$) [1]
C	IV	FBG-recoated	-5 000 to 7 500 [2]	5 000	2	N/A	N/A	N/A	N/A	N/A ($k_\varepsilon = 0.83$) [1]

[1] value provided upon request; [2] values from data sheet; delivered sensor is specified for an operating range of ±5 000 µm/m only

Table 2 shows that the specifications are fragmentary and inhomogeneous. Important parameters like hysteresis, information about linearity or repeatability are not available. Evaluation of the sensors is not possible without further information.
Also the information about wavelength to strain conversion is rather diverse. Manuf. A uses an individual calibration function (including temperature corrections) and provides the calibration parameters for each individual sensor, whereas manuf. B and C do not automatically provide any information to the user.
In order to verify the coefficients and to obtain information about the missing sensor specification (hysteresis, linearity, repeatability), we used our calibration facility (section 3) for testing the sensors.
Manuf. A and B use DTG's (draw tower gratings, produced by FBGS Technology) as sensing elements, which provide a very high strain limit (up to 50 000 µm/m, Chojetzki et al., 2004), at least for measurements over a short period. But as all the ready to use strain transducers listed in Table 2 are intended for long term use, the manufacturers conservatively specify the operating range as 15 000 µm/m as maximum. Manuf. C uses recoated FBGs and several 1 000 sensors of this type were installed across the world by different customers for SHM applications.

5. Strain calibration and results

Testing and calibration was carried out in order to find the most appropriate sensor for our application in the hydro power dam. There, surface mounting of the strain transducers is necessary. None of the manufacturers states a need for a specific supporting mechanism between the anchors in order to avoid bending out of the protective tube in the case of comparison. Thus we mounted the 0.5 m long sensors to the calibration facility without guiding.
For the calibration we have chosen a linear profile with equidistant spacing (steps of 500 µm/m) from zero strain to about 7 500 µm/m for sensor C (because of the recoated FBG) and about 10 000 µm/m for sensors A and B, see Tab.2.

Effect of the free fiber length

After the calibration measurements, the coefficients of the calibration function and additional sensor information are derived by comparing the fiber optic measurements (ε_{FOS}) to the interferometric reference measurements (ε_{Ref}). A value for L_F, which is needed for converting the ΔL values

measured by the interferometer to ε_{Ref}, is given for each of the sensors A with millimetre precision. For sensor B it is stated to be identical to L_A (pers. comm. with the manufacturer), and for sensor C L_F was estimated to be shorter for 15 mm than the measureable L_A by visible inspection (transparent protective tubing). ε_{Ref} changes for

$$d\varepsilon_{Ref} \approx \Delta L / L_F^2 \cdot dL_F \qquad (3)$$

with the uncertainty of the free fiber length dL_F. As an example, the error in strain is approx. 20 µm/m for a 0.5 m long sensor with an applied strain of 10 000 µm/m and a dL_F of 1 mm.

Nonlinearities

A typical result of the investigated strain transducers is shown in Figure 3, where the errors ($\Delta\varepsilon = \varepsilon_{Ref} - \varepsilon_{FOS}$) of the fiber optic system are shown. Here, ε_{FOS} was calculated using the instructions given by the manuf. for wavelength to strain conversion.

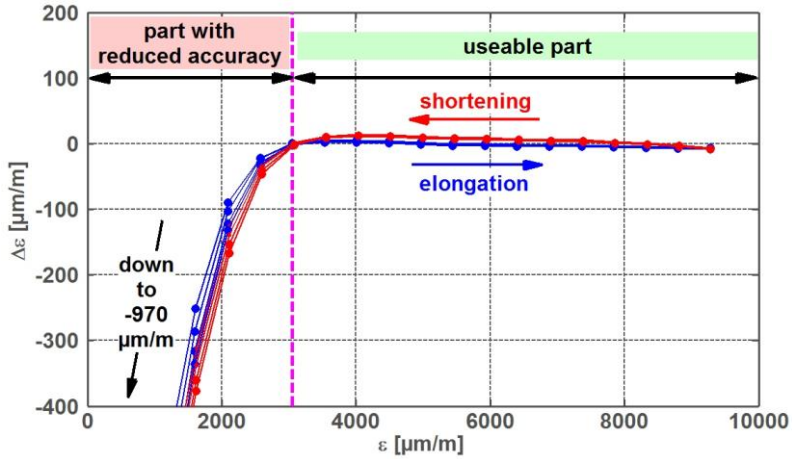

Figure 3: Calibration result of sensor A15 with a strong non-linearity in the lower strain region

Because of the strong non-linear part in the lower strain region we divide the whole strain range into a lower part with strongly reduced accuracy (deviations of up to some 1 000 µm/m) and an upper part with minor errors. The deviations in the lower part seem to be connected to the pre-tension of the fiber and may be caused by the deformation of the tubing, which tends to bend out at zero strain when a pre-strained sensor is compressed. A guiding mechanism of the tubing might reduce this effect, but such a mechanism is not recommended by any of the three manufacturers. Further investigations are necessary to investigate this effect.

Because of this effect, later the new calibration parameters were derived using data of the upper part only, see Tab. 3, and sufficient pre-straining is necessary during the installation as surface mounted sensors. The upper strain limit varies, as several sensors of manuf. A were arranged in chains, and spectral overlapping was avoided whilst measurement.

In order to investigate repeatability, the calibration run was repeated several times for all sensors.

Figure 4 shows the result of a sensor that was delivered without pre-tension. The strong non-linearity in the lower strain region does not appear for this sensor. Now, due to another scale of the figure, the hysteresis effect becomes more dominant, with a maximum deviation of 18 µm/m for the same ε_{Ref} reached either by lengthening or shortening the sensor. Hysteresis effects were observed for all investigated sensors.

Furthermore, the figure shows four calibration cycles and by this gives a good impression about the repeatability of this type of sensor which is < 4.7 µm/m.

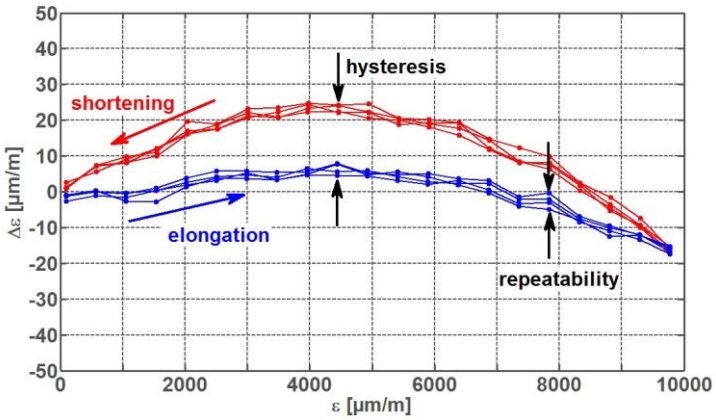

Figure 4: Calibration result of sensor B1 with a hysteresis effect and fluctuations due to repeatability

Several strain transducers of the same type

Another effect that can be seen in Figure 4 is the quadratic behaviour of the strain deviations, both for elongating and shortening the sensor. We now want to investigate this by means of a larger set of sensors. For this we split the 16 sensors of manuf. A into four groups of similar performance and exemplarily show the results of one sensor of each group, Figure 5a. For clarity, we only show one of the measured cycles for each sensor. The results shown were calculated using the individual calibration functions of the manufacturer. The two vertical lines in the plots (limit 1 and 2) indicate the starting position of the upper strain region, which is slightly different for the shown sensors. Data in the lower region are not shown.

The strain deviations of the sensors show different scale factors which result in measurement errors of up to 85 µm/m (Figure 5a) at a strain of about 9 000 µm/m. In order to eliminate these scale factors, we first estimated a linear calibration function for each sensor using least square adjustment. The resulting deviations are plotted in Figure 5b for the same set of sensors. The improvement of the individual calibration is evident, with a maximum deviation of 20 µm/m. Next, we applied a quadratic calibration function to the data of each sensor, and by this the deviations could be reduced again by a factor of 2, see Figure 5c. The maximum deviations are now originated by the hysteresis effects, which is about 10 µm/m for these sensors. Numerical values of the deviations are given in Tab. 3 for all three computation methods.

This example shows that calibration functions given by the manufacturer are of minor importance as long as the calibration range or the magnitude of the deviations is not specified. At the moment, individual calibration is still necessary if results of highest accuracy are needed.

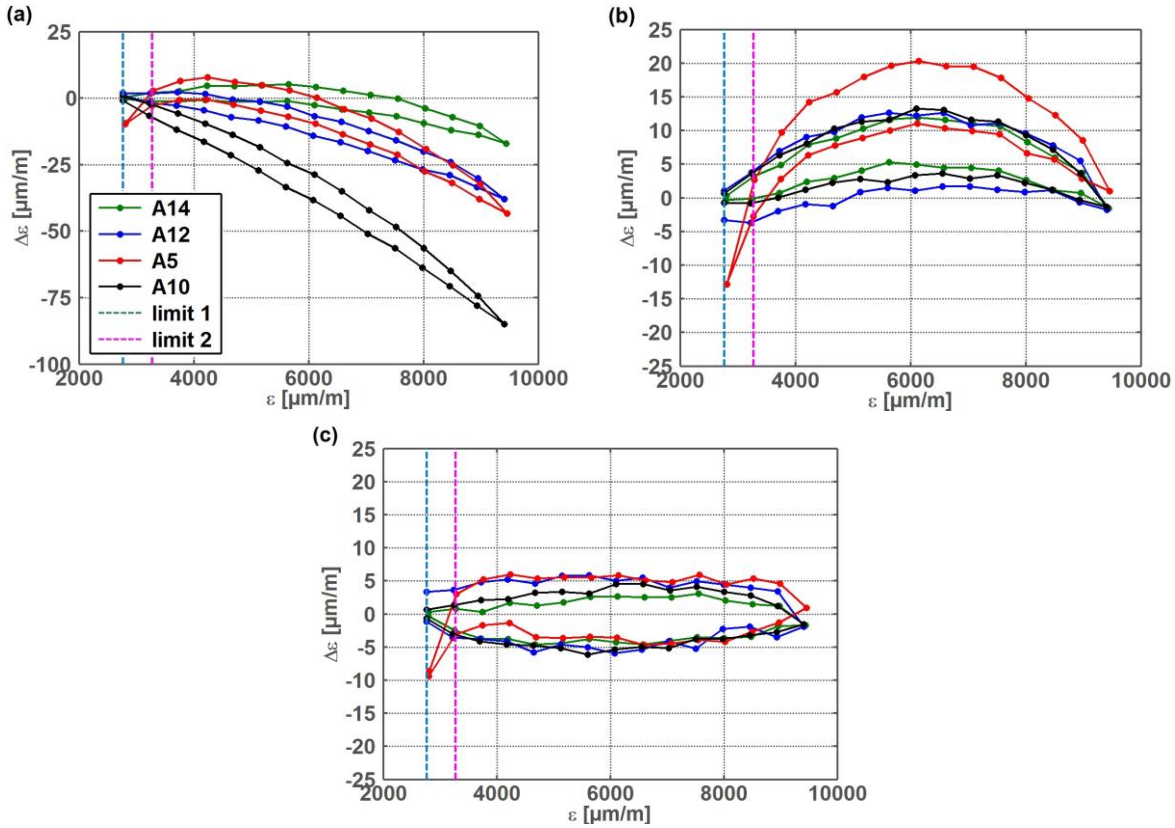

Figure 5: Sensor characteristics of a subset of sensors A (same sensors in all three plots) using (a) the calibration function provided by the manufacturer, or (b) an individually estimated linear or (c) a quadratic calibration function

Different types of strain transducers

Now we want to compare the performance of the different types of investigated sensors. As discussed before, the manufacturers use different calibration functions and in order to eliminate remaining non-linearities and scale errors, we apply our own calibration function (in this case the linear one) for this comparison. Figure 6 shows the results of four different sensor types. Again only one of the four measured cycles for each sensor is displayed.

All sensors show a large non-linearity in the lower strain region which might be a result of both, the construction details of the sensors and the pre-strain. Sensor B has the lowest pre-strain and sensor C has the largest one (about 5 000 µm/m). With no strain apparent, sensor C shows the largest deviations of about 2 000 µm/m, which is caused by the protective tube. It bends out for about 20 mm at the lower strain region and thus affects the measuring fiber. When the sensor is embedded, and by this the protective tube is guided by the surrounding concrete, this effect is not apparent any more. However, the results clearly show that the investigated sensors should be carefully used in applications, where surface mounting is necessary. Sufficient pre-strain must be applied during installation in order to avoid the erroneous low strain region. Thus, sensors without pre-strain are advantageous.

Measurements of higher accuracy can only be performed in the upper strain area, which's range is listed in Table 3 for all investigated sensors. But even in the upper strain area, all sensors show hysteresis effects with a quadratic behaviour of the strain deviations. Some of the sensors additionally show a significant scale effect in this region. When using the manufacturer calibration

function, the maximum strain deviation is 104 µm/m for the sensors A, 134 µm/m for the sensors B and 205 µm/m for sensor C, Table 3.

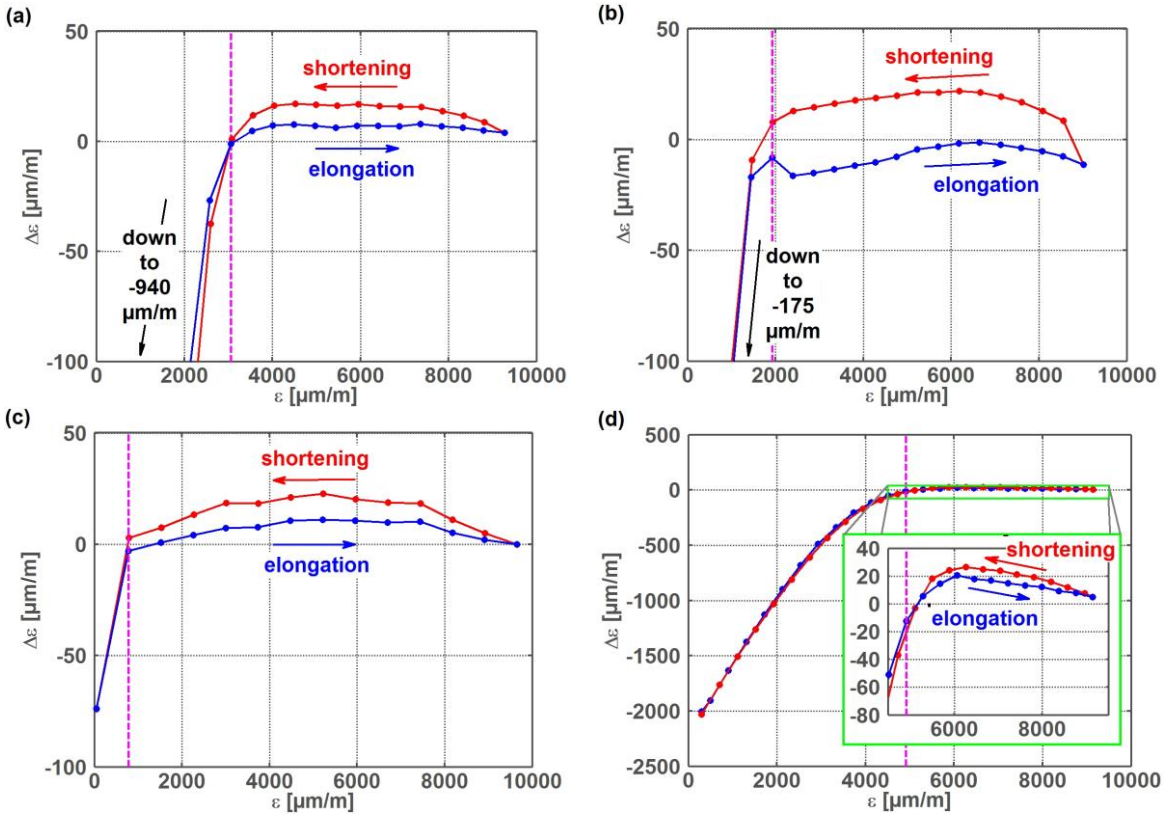

Figure 6: Strain deviations of different sensor types (surface mounted) after application of individual linear calibration functions; (a) sensor A15, (b) sensor A16, (c) sensor B2, (d) sensor C1

The strain deviations can be significantly reduced by applying an individual calibration function to the data in the upper strain region. Using a linear calibration function in accordance to Eq.2, the strain deviations could be reduced to 27 µm/m for the sensors A (type I). The estimated k_ε values are also listed in Table 3. They vary from 0.766 to 0.852 and one would suppose a rather good agreement with the values given in literature (see section 2). Only sensor C is out of this range, but it accords to the value specified by the manufacturer (0.83, Table 2). But because of the quadratic behaviour of the strain variations (Figure 6), k_ε is sensitive to the limit between the lower and the upper strain region, and k_ε also depends on the set-up of the sensor, where L_F is not known for all sensors (see section 4). Thus, this agreement is only of random nature and the individual calibration of strain transducers is necessary.

By using a quadratic calibration function, the strain deviations could be further reduced to 15 µm/m (sensors A, type I), which is now the magnitude of the hysteresis effect. These examples show that the individual calibration of the strain transducers gives a much higher performance compared to the manufacturer calibration, which can be seen for the other sensor types and the sensors of the other manufacturers (B1-3, C1) too.

The shown effects were the same when some experiments were repeated with another interrogator (different types and manufacturer compared) which clearly shows that the effects are caused by the individual strain transducers.

Table 3: Maximum deviation of the investigated sensors inside the upper strain part using different calibration functions

manufacturer	sensor		useable upper strain part (strain range used for calibration) from | to		maximum deviation inside the upper part, when using the manufacturer calibration function	maximum deviation inside the upper part, when using the linear calibration function	maximum deviation inside the upper part, when using the quadratic calibration function	k_ε estimated using a linear calibration function
	type	#	[µm/m]					[ ]
A	I	1	1802	8479	79.3	20.2	8.1	0.775
		2	3460	9159	27.1	18.2	10.1	0.775
		3	3241	9429	50.8	20.1	6.7	0.776
		4	3754	8988	28.0	12.8	7.2	0.777
		5	3268	9452	54.7	22.9	7.1	0.777
		6	4163	9402	40.6	16.9	8.7	0.771
		7	4177	9417	45.2	16.7	7.5	0.777
		8	2788	5630	20.2	12.6	7.7	0.770
		9	2753	9401	56.6	14.7	6.8	0.776
		10	2762	9410	88.0	16.6	6.5	0.777
		11	2972	9140	104.0	15.8	11.9	0.776
		12	3221	9407	42.7	14.4	7.7	0.779
		13	2743	8918	83.1	26.1	15.4	0.775
		14	2796	9436	20.4	15.4	5.0	0.775
		15	3053	9278	23.1	15.7	8.1	0.775
	II	16	1923	9017	55.0	38.8	22.9	0.766
B	III	1	95	9778	46.4	38.3	13.5	0.784
		2	782	9655	49.7	26.1	8.0	0.779
		3	273	9644	134.0	25.7	4.2	0.794
C	IV	1	4909	9141	129.0	26.7	24.2	0.852

6. Conclusion

The investigation of a variety of strain transducers of different manufacturers has shown large errors at small strains when using the calibration functions provided by the manufacturers. These are much larger than specified. Although all investigated sensors are intended for both, surface mounting and embedment, one must take special care (i.e. sufficiently pre-strain) when surface mounting. Sensors without or with a rather low pre-strain seem to be preferable for these applications.

Restricting the usable strain range to the more linear region and applying individual calibration functions, the maximum deviations could be reduced from several tens to hundreds of µm/m to $5 \leq \Delta\varepsilon \leq 25$ µm/m for the different sensors. One remaining effect is the hysteresis effect which is one of the main limiting factors of accuracy. Further investigation of this effect is necessary to clarify its source.

The strain sensitivity of the investigated strain transducers varies for $\Delta k_\varepsilon = 0.086$. Although the determined k_ε values are consistent with values given in the literature or the manufacturer (C), it

must be explicitly noted that k_ε depends on the individual set-up of a strain transducer type and the different materials used to manufacture it. Due to the quadratic behaviour of the strain deviations, it also depends on the calibration range when a linear calibration function is applied. In such situations, the calibration range should additionally be specified in order to allow error estimation. k_ε also depends on the free fiber length inside the strain transducer and thus L_F is an important information, when strain transducers are used to measure deformation. Therefore, this value should also be specified in the data sheet of a strain transducer.
The results of this investigation, and the fact that the specifications for the different types of strain sensors are rather inhomogeneous, shows the clear need for dedicated fiber optic standards which currently are under development (e.g. IEC 61757-2).

REFERENCES

BERGHMANS F. AND GEERNAERT T., Optical Fiber Point Sensors. In THÉVENAZ, L. (ED.), Advanced Fiber Optics: Concepts and Technology, EPFL Press, Lausanne, CH, 2011, pp. 309-344.

CHOJETZKI C., KLAIBERG T., OMMER J., ROTHARDT M., BETZ D., Faser-Bragg-Gitter für Hochtemperaturanwendungen. Technisches Messen 71, 2004, pp. 555-652.

HABEL W.R. AND SCHUKAR V.G., Validation of strain sensors to achieve reliable measurement results. Proc. 5th Int. Conf. on Structural Health Monitoring of Intelligent Infrastructure (SHMII-5), Cancún, México, 2011, 13 p.

IEC 61757-2-1, Fibre optic sensors – Part 2-1: Strain measurement – Strain sensors based on fibre Bragg gratings. Commitee Draft, 2014-07-11, 42 p.

INAUDI D., ELAMARI A., PFLUG L., GISIN N., BREGUET J., AND VURPILLOT S., Low-coherence deformation sensors for the monitoring of civil-engineering structures. Sensors and Actuators A 44, 1994, pp. 125-130.

JCGM, Evaluation of measurement data - Guide to the expression of uncertainty in measurement. JCGM Publ. 100: 2008, www.bipm.org, 134 p.

KASHYAP R. AND LÓPEZ-HIGUERA J.M., Fiber Grating Technology: Theory, Photosensitivity, Fabrication and Characterization. In LÓPEZ-HIGUERA J.M. (ED.) Handbook of Optical Fibre Sensing Technology. Wiley, 2002, pp. 349-377.

KLUG F., LIENHART W. AND WOSCHITZ H., High resolution monitoring of expansion joints of a concrete arch dam using fiber optic sensors. Proc. 6th World Conf. of the Int. Assoc. for Structural Control and Monitoring (IASCM), 2014, pp. 3164 – 3176.

OTHONOS A AND KALLI K., Fiber Bragg Gratings: Fundamentals and Applications in Telecommunications and Sensing. Artech House, Boston, 1999, 422 p.

PRESL R., Entwicklung eines automatisierten Messsystems zur Charakterisierung faseroptischer Dehnungssensoren. M.S. thesis, FH Oberösterreich, Wels, Austria, 2009, 148 p.

ROTHHARDT M., CHOJETZKI C. AND MUELLER H.R., High mechanical strength single-pulse draw tower gratings, Proc. SPIE Vol. 5579, 2004, pp. 127-135.

PETERS K., Fiber Bragg Grating Sensors. In BOLLER C. ET AL. (EDS.) Encyclopedia of Structural Health Monitoring, Vol.3., 2009, pp. 1097-1111.

SPILLMAN W.B. AND UDD E., Field Guide to Fiber Optic Sensors. SPIE Field Guides Vol. FG34, SPIE Press, Washington, USA, 2014, 134 p.

UDD E. AND SPILLMAN W.B., Fiber Optic Sensors: An Introduction for Engineers and Scientists. 2nd ed., Wiley, 2011, 512 p.

VDI/VDE STANDARD 2660-1: Optical strain sensor based on fibre Bragg grating - Fundamentals, characteristics and sensor testing, ICS 17.180.99, 33.180.10, Beuth Verlag, Berlin, 2010, 43 p.